

AD-A052 447

TULSA UNIV OK

F/G 17/9

RADAR SIGNATURES FOR AIRCRAFT IDENTIFICATION.(U)

FEB 78 R D STRATTAN

AFOSR-77-3200

UNCLASSIFIED

AFOSR-TR-78-0688

NL

| OF |

AD
A052447



END
DATE
FILMED
5-78
DDC

SECURITY CLASSIFICATION OF THIS PAGE (When Data Entered)

19. REPORT DOCUMENTATION PAGE		READ INSTRUCTIONS BEFORE COMPLETING FORM	
1. REPORT NUMBER 28 AFOSR-TR-78-0688	2. GOVT ACCESSION NO.	3. RECIPIENT'S CATALOG NUMBER	
4. TITLE (and Subtitle) Radar Signatures for Aircraft Identification	5. TYPE OF REPORT & PERIOD COVERED FINAL SCIENTIFIC REPT. Nov 1976 - Dec 1977		
7. AUTHOR(s) 10 Robert D. Strattan	8. CONTRACT OR GRANT NUMBER(s) 15 AFOSR-77-3200 new		
9. PERFORMING ORGANIZATION NAME AND ADDRESS University of Tulsa Tulsa, Oklahoma	10. PROGRAM ELEMENT, PROJECT, TASK AREA & WORK UNIT NUMBERS 61102F, 2305/D9 16 17 D9		
11. CONTROLLING OFFICE NAME AND ADDRESS Air Force Office of Scientific Research Electronic & Solid State Sciences / NE Bolling AFB, DC 20332	12. REPORT DATE 11 28 February 1978		
14. MONITORING AGENCY NAME & ADDRESS (if different from Controlling Office)	13. NUMBER OF PAGES 38 12 408		
	15. SECURITY CLASS. (of this report) UNCLASSIFIED		
	15a. DECLASSIFICATION/DOWNGRADING SCHEDULE		
16. DISTRIBUTION STATEMENT (of this Report) Approved for public release; distribution unlimited.			
17. DISTRIBUTION STATEMENT (of the abstract entered in Block 20, if different from Report)			
18. SUPPLEMENTARY NOTES			
19. KEY WORDS (Continue on reverse side if necessary and identify by block number)			
20. ABSTRACT (Continue on reverse side if necessary and identify by block number) A compact method of describing the radar scattering of distributed targets is developed. A computer program that processes the descriptor format into a target plane map of scattering intensity and forms simulated synthetic aperture radar images has been coded. Examples of aircraft and multiple reflection targets are shown.			

DD FORM 1 JAN 73 1473

EDITION OF 1 NOV 65 IS OBSOLETE

UNCLASSIFIED

SECURITY CLASSIFICATION OF THIS PAGE (When Data Entered)

DDC FILE COPY AD A 052447

DDC
APR 10 1978
F

393 175

JOB

Final Scientific Report

AFOSR Grant 77-3200

RADAR SIGNATURES FOR AIRCRAFT IDENTIFICATION

by

Robert D. Strattan

University of Tulsa
Tulsa, Oklahoma

February 28, 1978

Prepared for

Air Force Office of Scientific Research
Bolling AFB, D.C.

Approved for public release;
distribution unlimited.

PREFACE

This study has been sponsored by the Air Force Office of Scientific Research under grant AFOSR 77-3200. The work was performed at the University of Tulsa, Engineering Systems Division during the time period of November, 1976 to December, 1977. The project was a mini-grant follow-on to the study performed by the author at Rome Air Development Center during the Summer, 1976 under the USAF-ASEE Summer Faculty Research Program. The project involved approximately 2.1 person-months of the author's time.

The assistance of Bill Wolf of RADC/OCTM has been most helpful in acquiring reference material and providing guidance during the course of the project.

ACCESSION for	
NTIS	White Section <input checked="" type="checkbox"/>
RDC	Buff Section <input type="checkbox"/>
UNANNOUNCED	<input type="checkbox"/>
J.S. LOCATION	
BY	
DISTRIBUTION/AVAILABILITY CODES	
SPECIAL	
A	

ABSTRACT

A compact method of describing the radar scattering of distributed targets is developed. A computer program that processes the descriptor format into a target plane map of scattering intensity and forms simulated synthetic aperture radar images has been coded. Examples of aircraft and multiple reflection targets are shown.

TABLE OF CONTENTS

I.	Introduction	1
II.	Radar Signatures of Distributed Targets	3
III.	Descriptor Model for Distributed Targets	6
IV.	Imaging Radar Simulator	12
V.	Examples of Target Images	15
VI.	Conclusions	26
	References	27
	Appendix: Computer Program Description	28

LIST OF TABLES

III-1	Description Parameters for Open End Cylinder Target . . .	7
V-1	Description Parameters for Cone Cylinder Rocket Target .	18
V-2	Description Parameters for Aircraft Target	21
A-1	Functional List of Subprograms	30
A-2	Labeled Common Data Blocks	32

LIST OF FIGURES

III-1	Target Geometry for Open End Cylinder Target	8
III-2	Target Plane Distribution of Open End Cylinder Target at 45° Aspect Angle	11
V-1	Image of Open End Cylinder Target at 45° Aspect Angle.	16
V-2	Image of Open End Cylinder Target at 135° Aspect Angle	17
V-3	Image of Cone Cylinder Rocket Target at 170° Aspect Angle	20
V-4	Image of Aircraft Target at 165° Aspect Angle	23
V-5	Image of Aircraft Target at 100° Aspect Angle	24
V-6	Image of Aircraft Target at 45° Aspect Angle	25

I. INTRODUCTION

Developments in spread spectrum high resolutions imaging radar technology point toward the feasibility of a radar identifier. The radar would extract sufficient detail from the target's signature that the aircraft could be classified, perhaps to the level of a model designation. This classification and other information could then be used to identify the aircraft. A primary application for this concept would be for military surveillance radars. It could also have applications for civilian air traffic control systems.

Two basic approaches have been suggested for the radar identifier. The low frequency approach would use radar frequencies in the upper Rayleigh and lower resonance region to extract data on scattering modes related to volume and general shape. Typical frequencies would be in the VHF bands. The alternate approach uses microwave frequencies. The scattering is in the optics region and very shape dependent. These methods are discussed in References 1 and 4.

This study addresses the problem of predicting and analyzing signatures acquired by microwave imaging radars. The identification process requires the classification of an unknown target's signature through comparison to known signature features. The objective is to identify and model the dominant characteristics of scattering from aircraft targets and analyze their role in the classification and identification process.

A concept of modeling the scattering from a distributed target is presented. A digital computer program is used to simulate the images that would be produced by typical radars. The utility of the distributed target modeling concept is shown. Some of the complicating effects on imaging of scattering from non-specular targets are shown.

II. RADAR SIGNATURES OF DISTRIBUTED TARGETS

The radar signature of a target is quite complex and functionally dependent on many variables. The viewing direction of the radar, its frequency and polarization strongly affect signature features. The radar waveform and bandwidth also affect the information content of the signature.

The simplest form of a radar signature is the radar cross section. This is a single number at a frequency, aspect angle and polarization that describes the magnitude of the reflected signal. The returned signal strength is that which would be received if the incident radar power intercepted by an area equal to the radar cross sections were reradiated isotropically. The term scattering length is used to describe this parameter when dealing with field values rather than power densities.

The concept of radar cross section is inadequate when describing the acquired signal from a radar with a short slant range resolution. Short pulse or impulse methods as well as spread spectrum waveforms may be used to achieve resolutions significantly less than the target's length. The signature then becomes a description of the variations of radar cross section or scattering length with slant range over the extent of the target. This readily provides a method of locating regions of intense scattering activity, referred to as scattering centers. These can usually be associated with physical features of the target, such as a surface normal to the incident wave or an abrupt change in shape or material composition. This form of a signature is referred to as a Range Time Intensity (RTI) profile.

Coherent radars are also capable of providing the phase as well as the magnitude of the RTI profiles. If these profiles are acquired at a number of aspect angles, scattering centers can be isolated in the cross range dimension as well as in slant range. The magnitude and phase information is normally acquired in the rectangular complex format on two channels. The I and Q channels refer to the in-phase and quadrature-phase components. The cross range profile is formed by taking the Fourier transform of the scattered signals at a constant slant range with respect to the aspect angle change. A two dimensional image of the scattering center locations can then be formed in synthetic radar fashion by transforming the RTI I/Q data acquired by rotation of the target over each slant range cell. This is the concept of the imaging radar.

The modeling of the scattering from a target requires that both the slant range intensity variation and the phase variation with target rotation be simulated if imaging effects are to be studied. The approach used is to define a scattering length for each cell of a two dimensional grid representing the target plane. The cell size corresponds to the division of the axes of the image plane into discrete steps for processing by numerical methods.

Classical radar scattering methods normally provide only information on scattering lengths, not on distribution of scattering intensities over the physical extent of the target. An indepth study of this problem should be able to produce formulas and guidelines for estimating these distributions. This was beyond the scope of this investigation, however. The approach here has been to assume that through insight and experience some distribution relationship was available to describe the characteristic of the target's scatterers. A compact method for describing

the features of these scatterers is then developed.

This approach also provides for the description of multiple reflection scatterers. These scatterers are characterized by an initial scattering at a directly illuminated point, the diffracted ray being scattered by another scatterer, and so on until a portion returns to the viewing radar. A jet engine inlet duct is an example of a dominant scatterer of this type. The imaging process may place the scattering center image outside of the physical extent of the target. Examples of this are described in References 2 and 3.

III. DESCRIPTOR MODEL FOR DISTRIBUTED TARGETS

The model presented here provides a compact method of describing a target made up from multiple scatterers, each of which may be distributed over a defined region of the target plane. It also provides a method for modeling multiple reflection targets that appear to be delayed behind their initial scattering point.

This compact descriptor format is then processed by a subroutine of the computer program to calculate the scattering length of each cell of the target plane. A 64×64 , or 4096 cell target plane was used for this study, but it could be easily expanded if computer memory and processing time were available. The scatterer descriptor vector uses 19 parameters. One vector is required per scatterer within the target. Up to 20 scatterers were used in the implementation of this study, but any number within computer processing constraints could be used. The descriptor vector contains all information about spacial and angular variation of the scattering distribution. A fourth order Fourier series is used to describe angular variation, its order can be easily expanded also.

An example of the use of the descriptor model serves to describe its features. An open end cylinder target has been modeled in this manner. The value of the elements of the descriptor vectors are shown in Table III-1. The table is in the format of a worksheet for preparing data for entry into the computer. The geometrical arrangement is shown in Figure III-1.

The target is a cylindrical shell 20 units long and 10 units in diameter. It is closed at the $-y_T$ end and open at the $+y_T$ end. It is rotated about its midpoint. The radar waves are incident along the y_R

Table III-1

Description Parameters for Open End Cylinder Target

TARGET IMAGE WORKSHEET




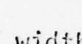
TARGET ID: 218.1FILE NAME: T1801

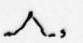
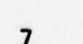
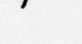


NO. OF SCATTERERS

NIS:

6

(20 MAX)

SCATTERER NO =		1	2	3	4	5	6	7	8	9	0
Scatter length GS		23	23	80	60	5	5				
0 = POINT											
1 = 	TX	1	1	2	2	1	1				
2 = 	TY	2	2	1	2	1	1				
3 = 	WX	10	10	5	5	1	1				
4 = 	WY	1	1	.5	1	1	1				
half width											
	XS0	5	-5	0	0	-5	5				
offset	YS0	0	0	-10	10	10	10				
rotation °	THS	-90	90	0	0	0	-90				
# of terms (0 to 4)	NF	4	4	4	4	4	4				
d.c. term	AF0	.14	.14	0	0	1.10	1.10				
cosine coefficients	AF (1)	.141	.141	.398	0	.413	.413				
	(2)	.147	.147	.027	0	0	0				
	(3)	.160	.160	.320	0	.05	.05				
	(4)	.160	.160	-.04	0	-.05	-.05				
sine coefficients	BF (1)	0	0	0	-.138	.413	.413				
	(2)	0	0	0	-.260	-.087	-.087				
	(3)	0	0	0	-.333	-.05	-.05				
	(4)	0	0	0	-.318	0	0				
delay distance	DLY	0	0	0	20	0	0				

Range filter: 0 = ideal, 1 = , 2 = , 3 = , 4 = , 5 = 

7

gaussion sin X/X sin X/X²

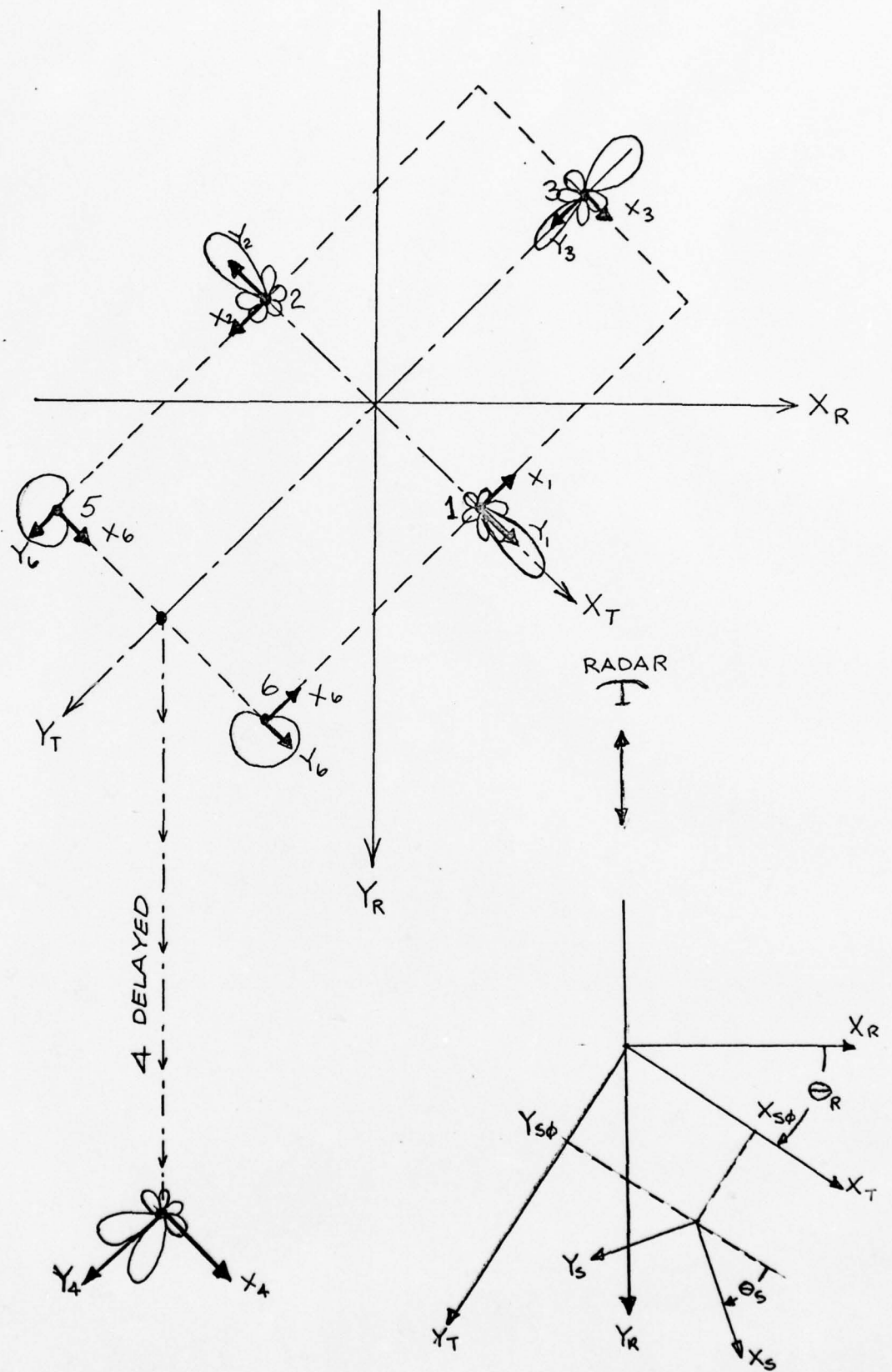


Figure III-1

Target Geometry for Open End Cylinder Target

direction and are backscattered in the $-y_R$ direction. The cross range coordinate is x_R and y_R is the slant range coordinate. The target is rotated by the angle θ_R . The radar will look directly into the cavity when $\theta_R = 180^\circ$.

The target is assumed to be composed of six scatterers. Scatterers 1 and 2 represent the broadside specular scattering from the cylindrical sides. Scatterer 3 is the flat plate scattering from the closed end. The main lobe is narrowed toward the $+y_T$ direction to account for shadowing by the cylindrical tube. Scatterer 4 represents the multiple bounce cavity echo due to waves diffracted into the cavity and subsequently reflected by the closed end termination. Scatterers 5 and 6 represent edge diffraction from the lips of the open cavity.

Each scatterer is given a scatter length, G.S. This is a measure of its intensity and can be calculated from classical radar cross section prediction formulas. The parameter TX and TY describe the variation of intensity with distance in the x_s and y_s directions. WX and WY are the half widths of the scatterers extent in the x_s and y_s direction. The scatterer's local coordinate system is translated by $x_{s\phi}$ and $y_{s\phi}$ from the target's origin, and rotated by THS. The cylinder broadside return simulated by scatterer 1 is assumed to be distributed uniformly in the x_1 direction and triangularly in the y_1 direction. It extends ± 10 units in x_1 and ± 1 unit in y_1 .

The angular variation of scattering intensity is described by a Fourier series. NF indicates the order of the series. All scattering intensities are scaled by the angular variation factor:

$$f = \frac{AF\phi}{2} + \sum_{i=1}^{NF} [AF(i) \cos(i\theta) + BF(i) \sin(i\theta)]$$

$$\text{where } \theta = \pi - \theta_s - \theta_R.$$

The angular variation is depicted by polar plots of f about the origin of each coordinate system in Figure III-1.

Multiple bounce scattering that is delayed due to the path length it must travel before returning to the radar is described by DLY, a delay distance. The scattering from the interior of the cavity is assumed to have traveled 20 units in a down and back path inside the cylinder before being reradiated back to the radar. It enters and leaves from the open end of the cylinder. Therefore scatterer 4 is given a DLY parameter of 20.

The processing algorithm proceeds on a cell by cell search over all the scatterers that make up the target to determine the scattering length of each cell. This is performed with the target rotated through the specified aspect angle. The resulting target plane scattering intensity map for the open end cylinder at an aspect angle of 45 degrees is shown in Figure III-2. The delayed scattering from the cavity can be seen down range from the cavity's mouth. This two dimensional array of scattering lengths is then available to study imaging radar processing effects or to use as a correlation mask in a target classification scheme.

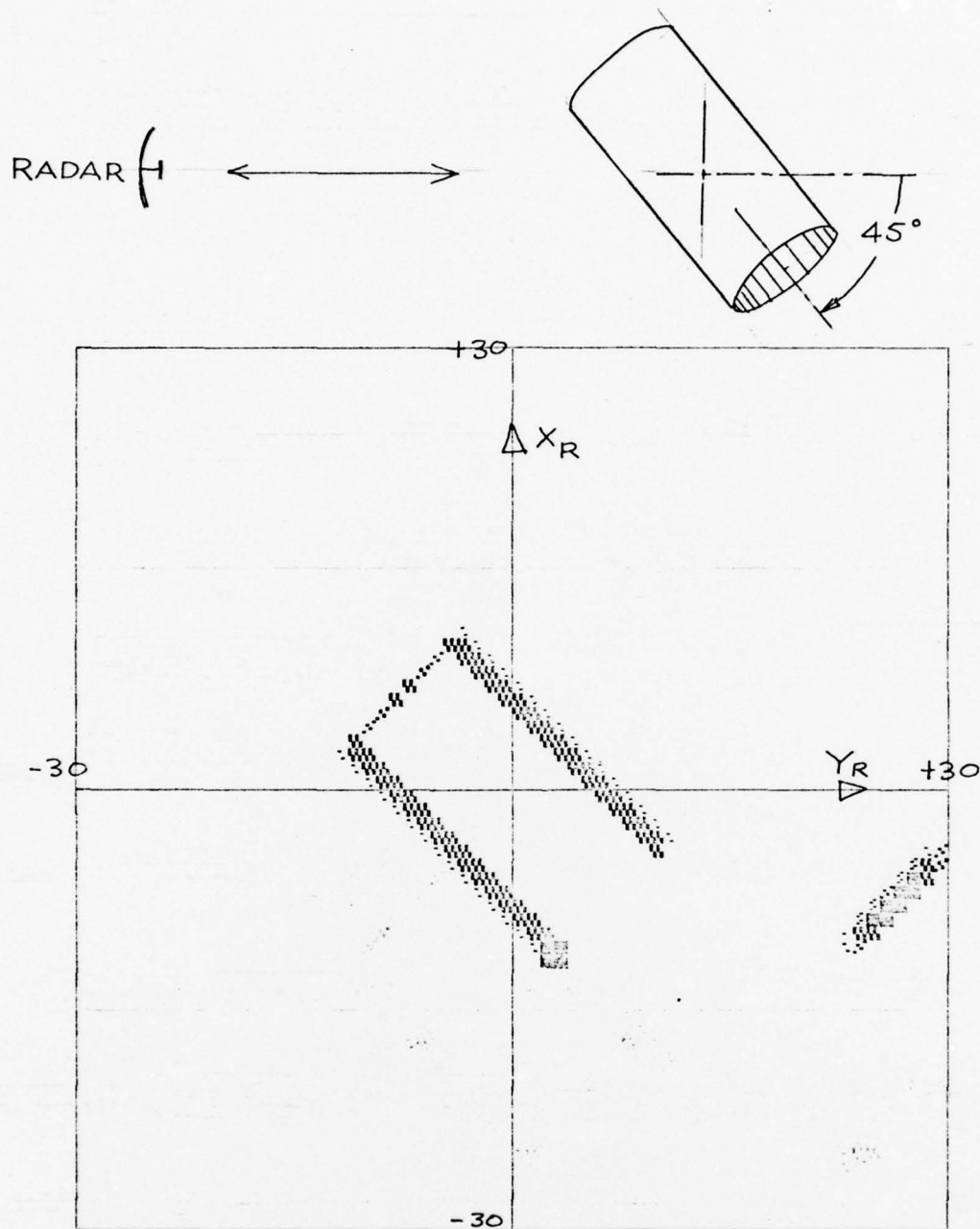


Figure III-2

Target Plane Distribution of Open End Cylinder Target at 45° Aspect Angle

IV. IMAGING RADAR SIMULATOR

A digital computer program that simulates the signal processing steps of an imaging radar has been written. The structure of this program as well as the subroutine for processing the elements of the target descriptor array are described in the Appendix. The imaging radar simulator uses the map of scattering lengths, such as that shown in Figure III-2, as its input.

The first step in the processing is to account for the finite range resolution capabilities of the radar. This is accomplished through the convolution of a range filter function with the scattering lengths along paths of fixed cross range location. This is then performed for each cross range cell increment until every cell value has been modified to account for the effect of range filtering.

If the scattering lengths are represented by elements S_{ij} before range filtering for the i th slant range cell and the j th cross range cell, and S'_{ij} after slant range filtering, the algorithm for range filter processing is:

for all i and j

$$S'_{ij} = \sum_k S_{kj} \cdot f(k-i)$$

$f(k-i)$ is a function defining the shape and extent of the range filter.

The length of the filter function and its shape are defined as input variables to the program.

A range time profile RTI) can be generated and output as a feature of the program. The value for the i th range cell is

$$R_i = \sum_j S'_{ij}$$

where the contribution for all scatterers at a constant range cell

increment are accumulated. An example of the RTI function is shown in Figure V-1.

The radar cross section is computed by accumulating the scattering contribution from each slant range cell of the RTI profile. The RCS is defined as

$$RCS = \sum_i R_i e^{\frac{-j4\pi y_c}{\lambda}}$$

where y_c is the cell size and λ is the wavelength.

An imaging radar must acquire doppler or phase change information in order to form the cross range profile. The simulation program computes this data immediately prior to transformation. A slant range interval is selected. A complex vector of 64 elements is computed from the j th row of the $[S'_{ji}]$ array of scattering lengths. The k th element of this vector corresponds to the I and Q channel outputs for the k th angular rotation increment of the target at the i th slant range cell.

$$C_k = \sum_j S'_{ji} e^{\frac{j[4\pi y_c}{\lambda} k\Delta]}$$

where Δ is the angular change between samples.

A weighting function is then applied to the C_k values. The Hamming function is normally used, but any defined function may be used.

The discrete Fourier transform of the weighted vector is then performed with a fast Fourier transform algorithm. The result is a cross range profile for the i th range increment. This operation is then repeated for each range increment until the entire target plane has been imaged.

The image is then normalized and plotted using a gray scale pattern to represent the imaged intensity for each target plane cell.

The calculation of the C vector and its subsequent Fourier transformation form a pair of operations that approximately reproduces the input data. However, the effect of the weighting function and the quantization of the data introduce effects unique to imaging radar. This also provides a point for injecting other real life limitation to imaging radar such as noise and jitter in the angular sampling increments. The study of these effects were beyond the scope of this study, but could be easily studied in the future using this algorithm.

V. EXAMPLES OF TARGET IMAGING

Several targets have been selected to demonstrate the features of this target description and image simulation technique. The scope of the program did not allow a detailed development of accurate models. The scatterer description parameters were selected more to demonstrate features of the method rather than to accurately simulate the scattering from an actual target.

The open end cylinder illustrates the multiple reflection effect found in cavity-type targets. Its description parameters were discussed in Section III. Images produced by the simulation program are shown in Figures V-1 and 2. The RTI profile is also shown in Figure V-1. At the 45° aspect angle of Figure V-1, the radar illuminates the closed end. The energy diffracted by the lip of the open end and traveling down the interior of the cylinder to be reflected back and then diffracted back to the radar by the lips shows up on the image some distance downrange from the cylinder. At 135° aspect angle, this interior cavity echo is stronger and appears down range from the mouth of the cavity. This is a similar effect to that described in Reference 3 for a space object shroud.

Reference 2 describes another form of multiple reflected waves where the diffracted waves are on the exterior of the body. A simple 7 scatterer model of a cone cylinder rocket has been defined in Table V-1. Scatterer 1 is the nose tip diffraction. Scatterers 2 and 3 represent the direct reflection from the cone-cylinder join. Scatterers 4 and 5 represent multiple bounce scattering from the cone-cylinder join to the aft cylinder termination back to the cone-cylinder join. Scatterer 6 and 7 represent the direct scattering from the aft cylinder termination.

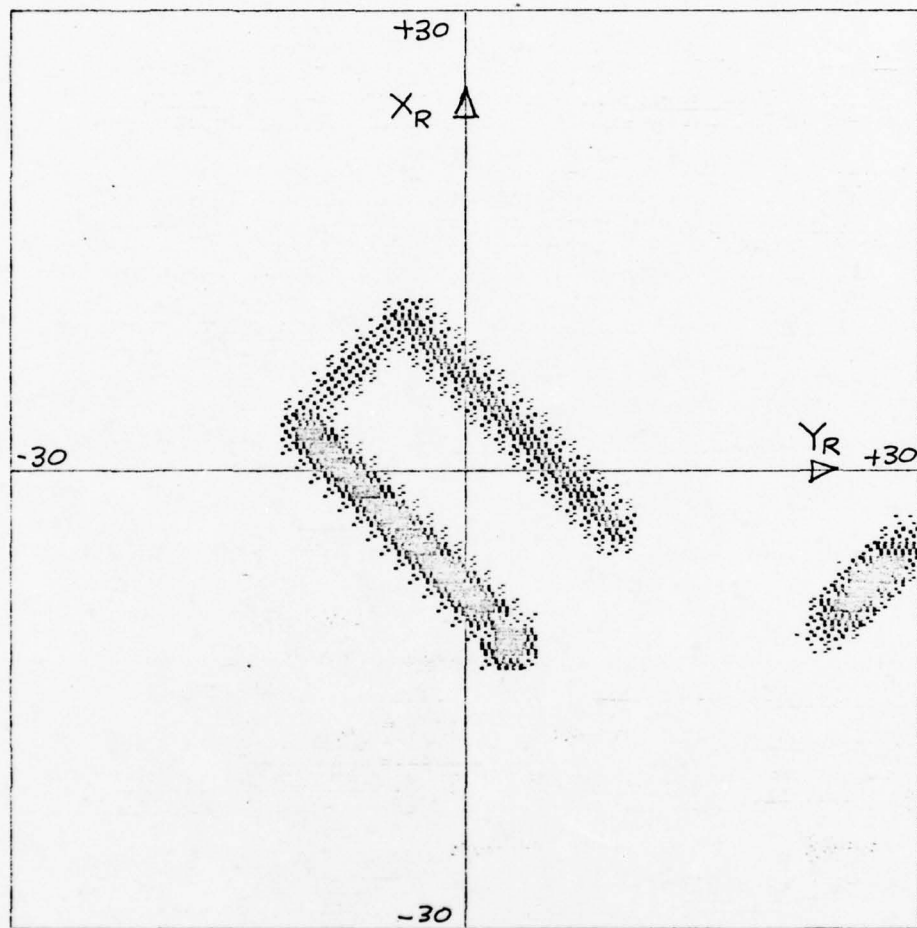
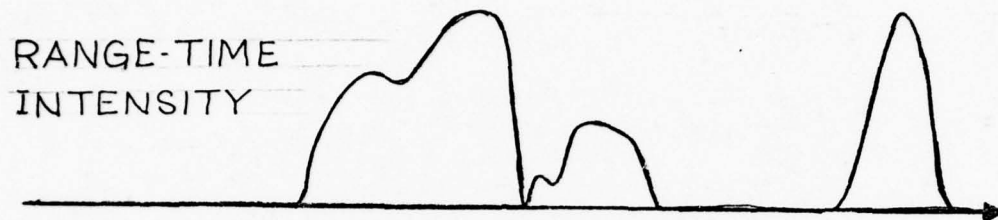


Figure V-1

Image of Open End Cylinder Target at 45° Aspect Angle

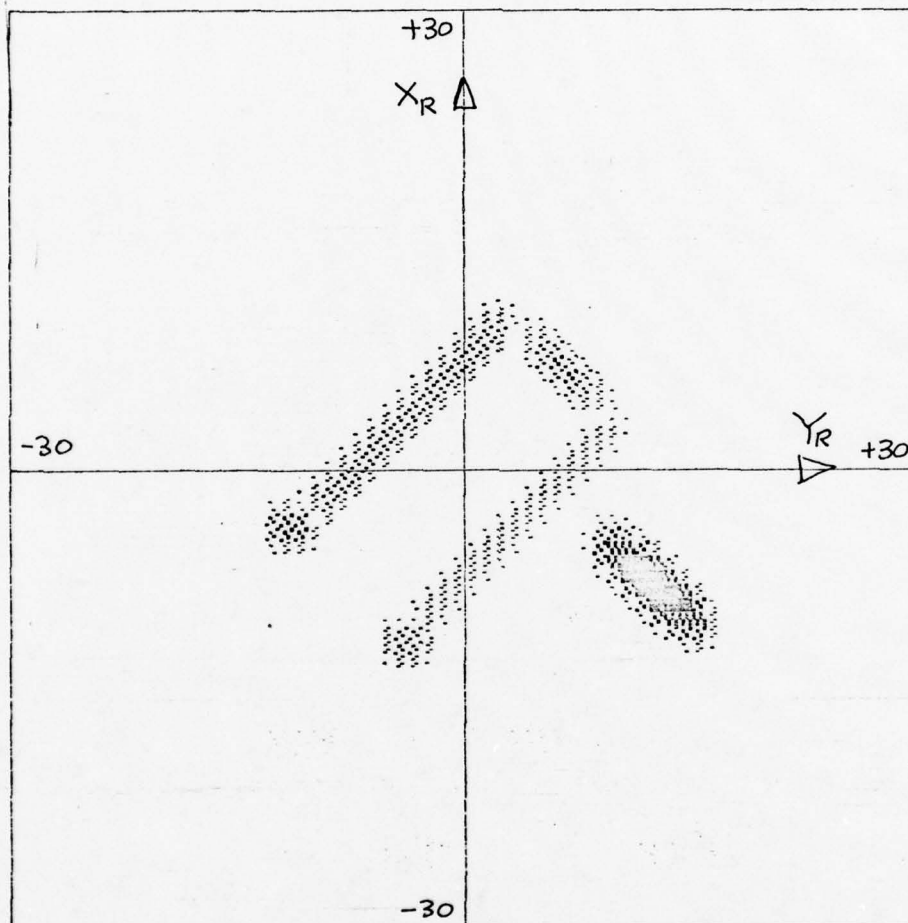


Figure V-2




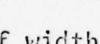
Image of Open End Cylinder Target at 135° Aspect Angle

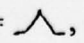
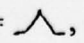
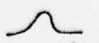
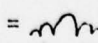
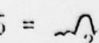
Table V-1

Description Parameters for Cone Cylinder Rocket Target

TARGET IMAGE WORKSHEET

TARGET ID: 26.3FILE NAME: T2603NO. OF SCATTERERS HS: 7 (20 MAX)

SCATTERER NO =		1	2	3	4	5	6	7	8	9	0
Scatter length GS		10	10	10	10	10	10	10			
0 = POINT											
1 = 	TX	2	2	2	2	2	2	2			
2 = 	TY	2	2	2	2	2	2	2			
3 = 	WX	1	1	1	1	1	1	1			
4 = 	WY	1	1	1	1	1	1	1			
half width											
offset	XSD	0	-3	3	-3	3	3	-3			
	YSD	15	10	10	10	10	-8	-8			
rotation °	THS	0	0	0	0	0	90	180			
# of terms (0 to 4)	NF	4	4	4	4	4	4	4			
d.c. term	AF0	.633	.633	.633	.633	.633	1.067	1.067			
cosine coefficients	AF (1)	.510	.510	.510	.510	.510	.419	.419			
	(2)	.233	.233	.233	.233	.233	0	0			
	(3)	0	0	0	0	0	.067	.067			
	(4)	-.067	-.067	-.067	-.067	-.067	-.053	-.053			
sine coefficients	BF (1)	0	0	0	0	0	.419	.419			
	(2)	0	0	0	0	0	-.056	-.056			
	(3)	0	0	0	0	0	-.067	-.067			
	(4)	0	0	0	0	0	0	0			
delay distance	DLY	0	0	0	18	18	0	0			

Range filter: 0 = ideal, 1 = , 2 = , 3 = , 4 = , 5 = 

gaussian sin X/X sin² X/X²

The image for a 170° aspect angle is shown in Figure V-3. An outline of the rocket has been superimposed. The radar views the rocket 10° from nose-on. The multiple reflected waves produce images directly down range from the cone-cylinder joins. One of these falls outside of the physical boundaries of the target.

An aircraft target is described by 14 scatterers in Table V-2. The aircraft is of the general configuration of a Lear-Jet. Scatterer 1 and 2 represent the nose radar and cockpit areas. The engine inlet ducts are scatterers 3 and 4 while the engine exhaust ducts are scatterers 5 and 6. The tail surfaces are scatterers 7 and 8. Wing tip tanks are scatterers 9 and 10 while the fuselage broadsides are scatterers 11 and 12. Wing edges are represented by scatterers 13 and 14.

The aircraft's image is shown at three viewing angles in Figures V-4, 5 and 6. The radar viewing angle is 15° from nose-on in Figure V-4. The nose area, one wing and the illuminated engine inlet are the dominant scatterers. The forward fuselage broadside and the illuminated engine inlet are dominant at the near broadside view of Figure V-5. The engine exhaust ducts are the most intense scatterers at the rear quarter view of Figure V-6.

The aircraft example illustrates the ability to model the effects of viewing angle on radar images. The intensity of many scattering centers change drastically with a aspect angle. The Fourier series approach appears effective. Higher order terms are needed to allow for more rapid angular variation, however.

Time limitation and the scope of the program have prevented any indepth attempts at more realistic modeling of actual targets.

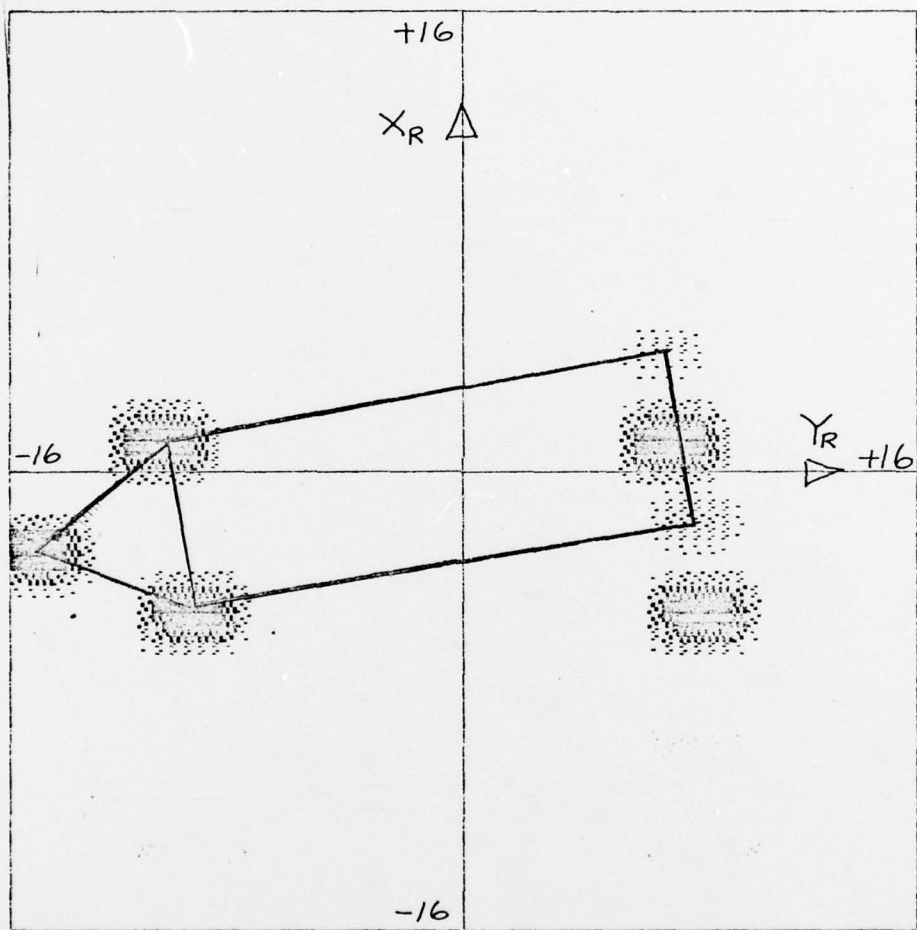


Figure V-3

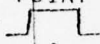


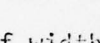
Image of Cone Cylinder Rocket Target at 170° Aspect Angle

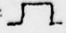
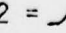
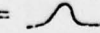
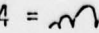
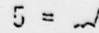
Table V-2

Description Parameters for Aircraft Target

TARGET IMAGE WORKSHEET

TARGET ID: 26.2FILE NAME: T2602NO. OF SCATTERERS HS: 14 (20 MAX)

SCATTERER NO =		1	2	3	4	5	6	7	8	9	10
Scatter length	GS	10	10	10	10	10	10	2	2	10	10
0 = POINT	TX	2	2	1	1	1	1	2	2	2	2
1 = 	TY	1	2	1	1	1	1	1	1	2	2
2 = 	WX	2	4	2	1	2	2	5	5	5	5
3 = 	WY	2	2	1	2	1	1	3	3	2	2
4 = 	XS0	0	0	6	-6	6	-6	5	-5	18	-18
half width	YS0	28	20	-4	-4	-12	-12	-20	-20	2	2
offset	THS	0	0	0	90	180	180	-30	30	-90	90
rotation °	NF	4	4	4	4	4	4	4	4	4	4
# of terms (0 to 4)	AF0	.633	1.167	.667	.667	.633	.633	0	0	.167	.167
d.c. term	AF (1)	.510	.622	.394	.394	.510	.510	.333	.333	.167	.167
cosine coefficients	(2)	.233	-.167	0	0	.233	.233	0	0	.167	.167
	(3)	0	-.167	0	0	0	0	.333	.333	.167	.167
	(4)	-.067	.167	.167	.167	-.067	-.067	0	0	.167	.167
sine coefficients	BF (1)	0	0	-.394	-.394	0	0	0	0	0	0
	(2)	0	0	-.289	-.289	0	0	0	0	0	0
	(3)	0	0	0	0	0	0	0	0	0	0
	(4)	0	0	0	0	0	0	0	0	0	0
delay distance	DLY	0	0	0	0	0	0	0	0	0	0

Range filter: 0 = ideal, 1 = , 2 = , 3 = , 4 = , 5 = 

gaussian sin X/X sin² X/X²

Table V-2 (cont.)

Description Parameters for Aircraft Target

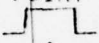


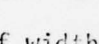
TARGET IMAGE WORKSHEET

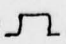

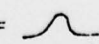
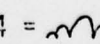
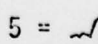
TARGET ID: 26.2FILE NAME: T 2602

NO. OF SCATTERERS

HS: 14

(20 MAX) (CONT.)

SCATTERER NO =		11	12	13	14	5	6	7	8	9	0
Scatter length	GS	20	20	20	20						
0 = POINT	TX	2	2	1	1						
1 = 	TY	1	1	1	1						
2 = 	WX	10	10	6	6						
3 = 	WY	2	2	1	1						
4 = 	XSØ	2	-2	10	-10						
half width	YSØ	18	18	7	7						
offset	THS	-90	90	-30	30						
rotation °	NF	4	4	4	4						
# of terms (0 to 4)	AFØ	.167	.167	.167	.167						
d.c. term	AF (1)	.167	.167	.167	.167						
cosine coefficients	(2)	.167	.167	.167	.167						
	(3)	.167	.167	.167	.167						
	(4)	.167	.167	.167	.167						
sine coefficients	BF (1)	0	0	0	0						
	(2)	0	0	0	0						
	(3)	0	0	0	0						
	(4)	0	0	0	0						
delay distance	DLY	0	0	0	0						

Range filter: 0 = ideal, 1 = , 2 = , 3 = , 4 = , 5 = 

gaussian sin X/X sin² X/X²

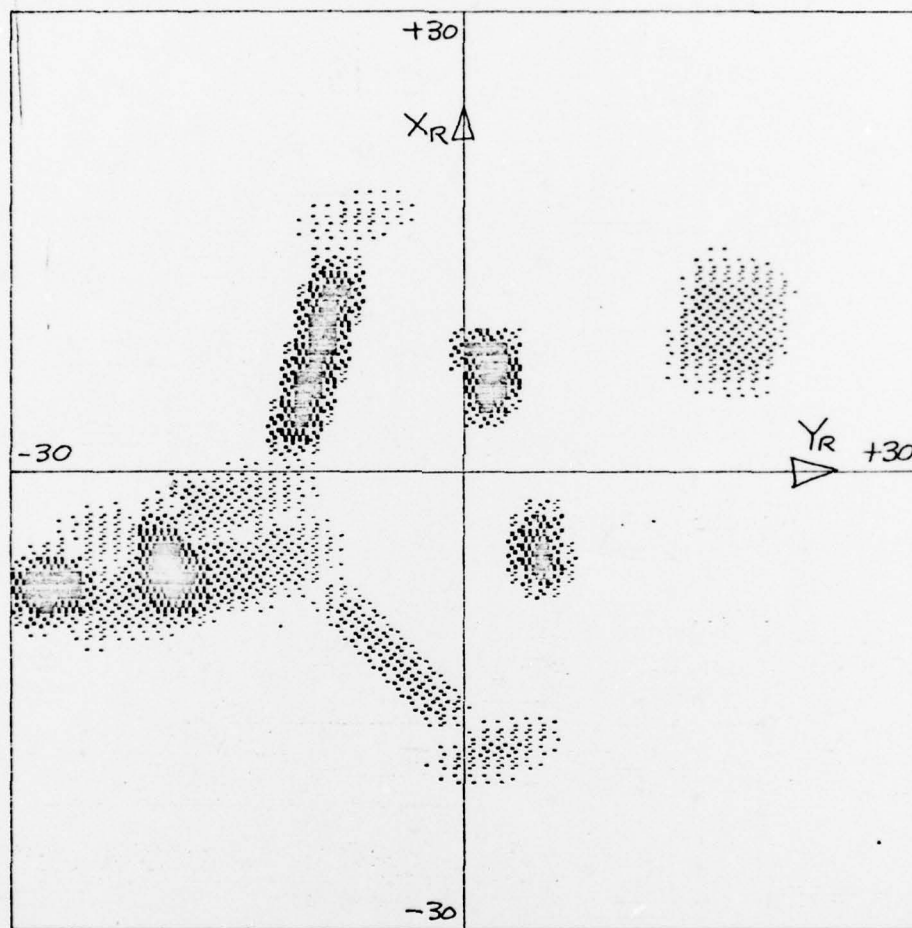


Figure V-4

Image of Aircraft Target at 165° Aspect Angle

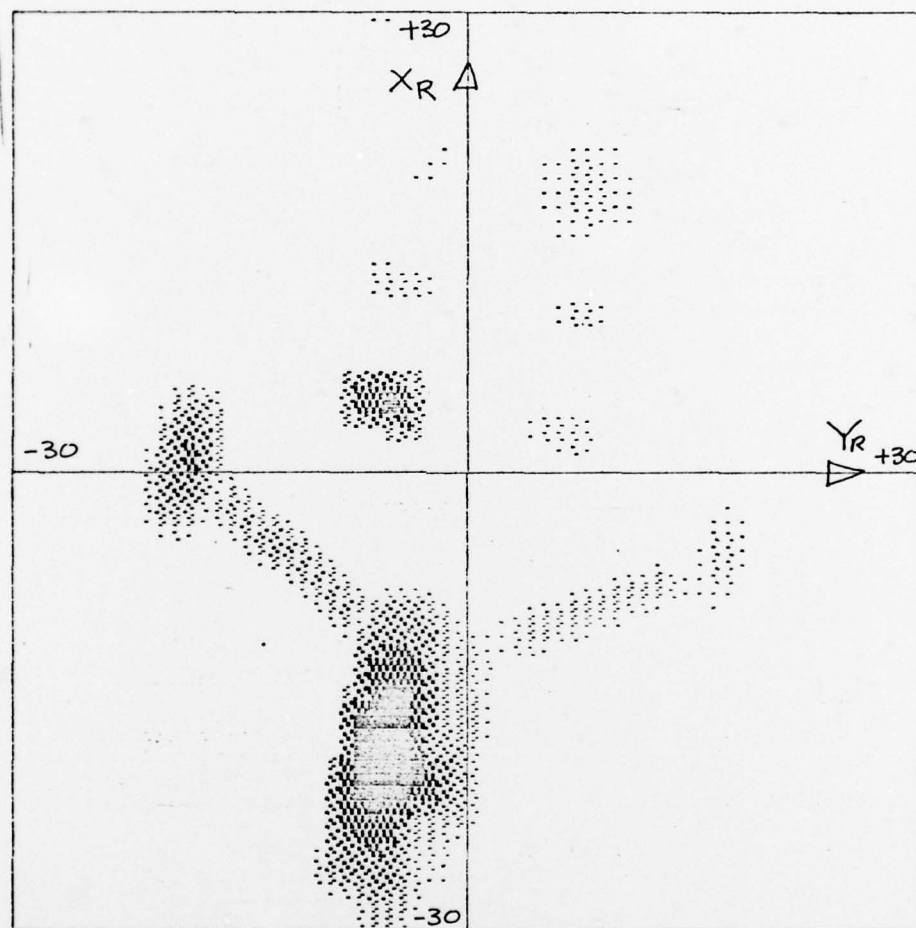


Figure V-5

Image of Aircraft Target at 100° Aspect Angle

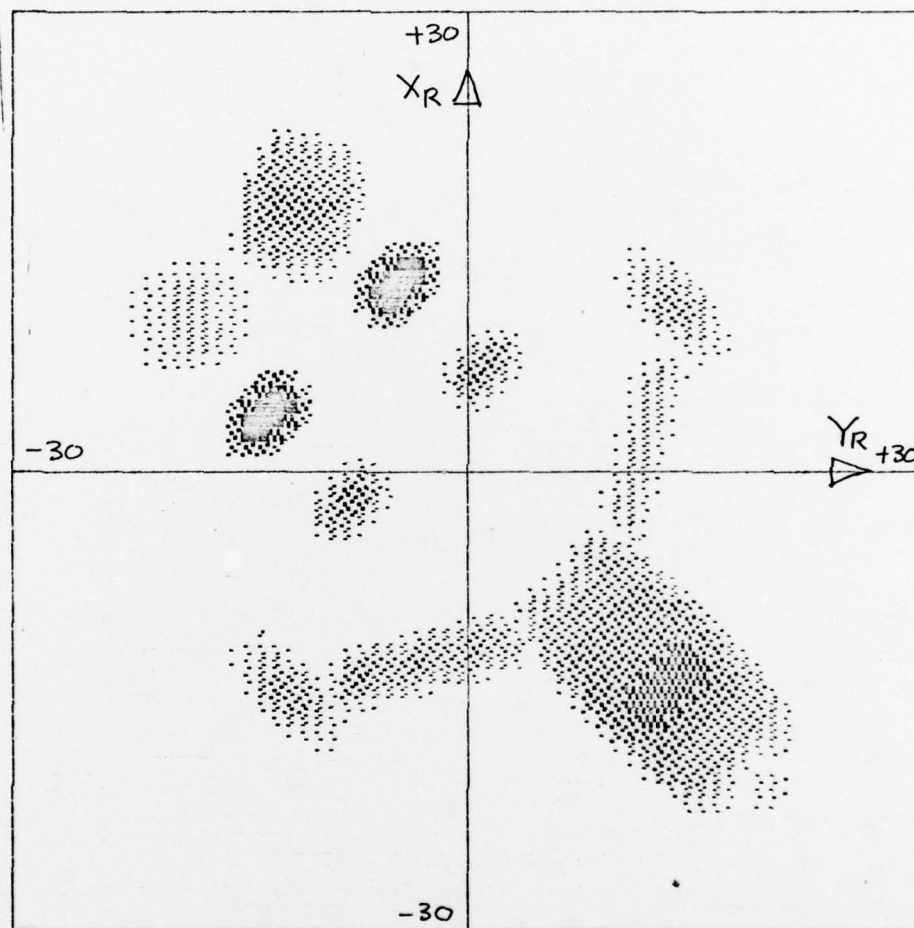


Figure V-6

Image of Aircraft Target at 45° Aspect Angle
Wavelength $\approx .0469$, Rotation angle = 1.43 degrees,
Range filter: triangular, 3.75 total length

VI. CONCLUSIONS

The overall objective has been to model the microwave region radar scattering from aircraft targets and to investigate imaging and identification anomalies arising in real-life situations. The scope of this short study has been limited to the development of a compact descriptor model for target scattering and the coding of a digital computer program that produces simulated radar images.

Targets composed of many scattering centers are described by a set of descriptor vectors. Each vector corresponds to a scatterer and accounts for the physical extent, spacial variation and angular variation of the scatterer. A delay factor can also be introduced to account for multiple reflections.

A computer program that allows viewing a target at any aspect angle, accounts for range resolution effects and produces a synthetic aperture image of the target has been written. Several examples of target description and imaging have been shown.

The scope of the program prevented indepth analysis of real targets. However the mechanism now exists and could prove useful in future studies of imaging radars and identification schemes. The refinement of the method of modeling aircraft targets with more quantitative and accurate descriptors is recommended as a next step in this study.

REFERENCES

1. Real-World Limitation of Radar Signatures for Target Identification, R. D. Strattan, Participant's Final Report for 1976 USAF-ASEE Summer Faculty Research Program, Rome Air Development Center, Griffiss AFB, New York, August 13, 1976.
2. Radar Scattering Effects from Wideband Measurements and Coherent Processing, A.J. Moceyunas and R. F. Wallenberg, National Conference on Electromagnetic Scattering, University of Illinois at Chicago Circle, June 15-18, 1976.
3. Wideband Data Reductions for Electromagnetic Imaging, Analysis of Pegasus Shroud Model (U), R. F. Wallenberg, SURC TR73-277, August, 1973. Unclassified Sections I, II, III and V.
4. "Target Identification from Radar Signatures", R. D. Strattan, to be presented at the 1978 International Conference on Acoustics, Speech, and Signal Processing, April, 1978, Tulsa, Oklahoma.

A P P E N D I X

COMPUTER PROGRAM DESCRIPTION

The program used to implement the distributed target model and simulate high range resolution synthetic aperture imaging radar processing is described. The program is written in Fortran and implemented on an Interdata Model 70 minicomputer.

The program uses about 1000 lines of source text. The compiled program and the associated labeled common area require about 60 kilobytes of core. Execution time is under two minutes per scatterer. Program listings are available from the author on request.

The minicomputer has 64 kilobytes of core, a dual disc cartridge unit, four tape drives, a line printer and a Varian electrostatic printer/plotter.

The subprograms that make up the composite program are described in Table A1. The associated data blocks contained in labeled common area are described in Table A2. A description of a typical problem execution follows. The results are shown in examples described in the main body of the report.

The main control function enables selection of an exit from the program, target file input/output manipulation, radar parameter definition, problem definition, or the plotting of a gray scale test pattern. Normal operation begins by selecting the target input/output function.

The operator can build a target file, edit an existing file, print a file's contents on the printer, call a file from the disc, or save a file on the disc. A file may contain up to twenty scatterers. Each scatterer

is described by nineteen variables that specify its orientation, distribution and angular variation.

Radar parameter definition includes specifying the image plane size, angular rotation interval, range filter shape and extent, and wavelength. The problem is defined by specifying the aspect angle at which the radar views the target, pre-transformation weighting function selection, and the selection of output options.

Selection of the run mode initiates the calculation process. The GEOTGT subroutine generates a 64 x 64 cell map of scattering intensity on the slant range - cross range plane. The contribution of each distributed scatterer is superimposed on the image plane.

An image of this unprocessed target map may be plotted. A range-time profile prior to any radar filtering may be printed, also. The slant range filter response is then convolved with the target map to incorporate the effect of finite radar bandwidth. A range-time profile and image of the post-filtered target is also available, if selected.

The synthetic aperture processing then is performed. A slant range cell is selected. The cross range profile is converted to a vector of I/Q channel elements, each element corresponding to a sample at equally spaced small aspect angle intervals. This vector is then transformed using a fast Fourier transform algorithm. The transformed vector corresponds to the cross range profile of the target scattering lengths. This process proceeds through the range of the slant range cells to cover the full extent of the target. The result is a simulation of the image produced by a synthetic aperture radar. This image is then plotted.

TABLE A1
FUNCTIONAL LIST OF SUBPROGRAMS

MAIN	Calling program for overall control with menu of 5 operational modes.
TARGET	Subroutine to control BLK2 target file manipulation with menu of 5 operation modes.
SCATIN	Subroutine to manipulate the elements of an individual scatterer BLK 1 descriptor vector.
RADAR	Subroutine to acquire the radar system describing parameters.
PROB	Subroutine to acquire problem definition parameters.
RUN	Subroutine to control the execution of the calculation subprograms.
GEOTGT	Subroutine to generate the BLK4 scattering length composite map of a target composed of a set of scatterers. The descriptor vector of each scatterer in BLK 2 is processed through geometrical transformations to produce a map of the scattering lengths for each cell of the image plane.
RFLT	Subroutine to add the effect of finite radar bandwidth to the BLK 5 slant range signatures.
VPLT	Subroutine to plot a gray scale image of the BLK 4 array on the Varian electrostatic printer-plotter.
CR	Subroutine to generate I/Q records at a selected slant range cell. The cross range profile from the BLK 4 array is processed to generate 64 I/Q elements in BLK 7 array corresponding to 64 echoes at equally spaced aspect angle intervals.
FTDB	Subroutine to take the discrete Fourier transform of the BLK 7 array. The result is converted to decibel values and stored back in the corresponding row of the BLK 4 array.
NORM	Subroutine to normalize the BLK 4 array relative to the value of its maximum element value prior to image plotting.
OUT	Subroutine to control the output of data to the line printer and printer/plotter.
SLTR	Subroutine to compress the BLK 4 target map into a 64 element BLK 5 slant range profile.

Table A1, Functional List
of Subprograms (Continued)

RCS	Subroutine to calculate the long pulse radar scattering length from the BLK 5 slant range profile.
COOL 80	Subroutine to do fast Fourier transforms
PLCR	Subroutine to plot gray scale test pattern on the printer/plotter.

TABLE A2
Labeled Common Data Blocks

BLK1	20 element real array. Individual distributed scatterer descriptor array used during target file preparation
BLK2	$20 \times 20 + 2 = 402$ element real array. Target descriptor data file for up to 20 scatterers plus target 10 no. and number of scatterers in target.
BLK3	5 element real array. Logical unit assignments and value of pi and radian conversion constant.
BLK4	$64 \times 64 = 4096$ element real array. Storage of scattering lengths or image intensities of target plane cells. The rows correspond to slant range cells and the columns correspond to cross range cells.
BLK5	64 element real array. Range time profile of scattering lengths. The elements correspond to slant range cells.
BLK6	9 element real array. File of parameters defining the radar and processing parameters.
BLK7	65 element complex array. Input and output vector for the discrete Fourier transform algorithm